Scanning Microscopy

Volume 1994
Number 8 *The Science of Biological Microanalysis*

Article 7

3-22-1994

Improvements in Biological X-Ray Microanalysis: Cryoembedding for Specimen Preparation and Multivariate Statistical Analysis for Data Interpretation

C. Quintana
INSERM, France

N. Bonnet
University of Reims, France

Scanning Microscopy Supplement 8, 1994 (pages 83-99) 0892-953X/94$5.00+.25
Scanning Microscopy International, Chicago (AMF O'Hare), IL 60666 USA

IMPROVEMENTS IN BIOLOGICAL X-RAY MICROANALYSIS: CRYOEMBEDDING FOR SPECIMEN PREPARATION AND MULTIVARIATE STATISTICAL ANALYSIS FOR DATA INTERPRETATION

C. Quintana[1,2*] and N. Bonnet[3]

[1]INSERM, France, [2]Centro Nacional de Microelectrónica/CSIC, Madrid, Spain,
[3]INSERM U 314 and University of Reims, Reims, France

(Received for publication September 29, 1993, and in revised form March 22, 1994)

Abstract

For biological X-ray microanalysis, cryoembedding (CE) combined with cryofixation (CF) and cryodehydration (CD) was already proposed as an alternative method to freeze-dried cryosections in 1984 by Wróblewski and Wroblewski. CD by freeze-drying (FD) is usually recommended because it provides better retention of diffusible elements. CD by freeze-substitution (FS) has the advantage of being simpler, giving more reproducible preservation of ultrastructure and causing fewer problems for resin infiltration. We have increased the retention of diffusible elements by using home-made devices for CS and CE in the new Lowicryl K11M and HM23 resins. These resins allow samples to be kept at a maximum temperature of 213K and 193K respectively.

Application of multivariate statistical analysis (MSA) to X-ray data (spectra and maps) allows the study of correlations between the analyzed elements in different nuclear areas and in the cytoplasm. The "factorial" images, obtained with MSA, display the compartments of strong correlation between P and K (nucleic acids) and the compartments of strong correlation between S and K (proteins). We suggest that the future application of MSA methods will provide increased knowledge of the physio-pathological compartmentation of diffusible elements at the subcellular level.

Key words: Cryofixation, freeze-substitution, Lowicryl HM23 cryoembeddding, X-ray mapping, multivariate statistical analysis

*Address for correspondence:
C. Quintana,
Centro Nacional de Microelectrónica/CSIC,
Serrano 144, 28006 Madrid, Spain
Telephone number: +34-1-5625311
Fax number: +34-1-4117651

Introduction

Freeze-drying of cryosections (FD/CS) of cryofixed material is the cryomethod classically used for X-ray microanalysis of biological specimens. Cryoembedding (CE) in Lowicryl resins combined with cryofixation (CF) and cryodehydration (CD) (freeze-drying (FD) or freeze-substitution (FS) was proposed as an alternative method to FD/CS by Wróblewski and Wroblewski (1984). Freeze-drying is usually recommended because it provides better retention of diffusible elements. However, freeze-substitution has the advantage of being simpler, it provides reproducible preservation of the ultrastructure and causes fewer problems for resin infiltration.

The interest in such a set of cryotechniques has increased since 1985 after the emergence of the new Lowicryl resins K11M and HM23 which allow the investigator to keep samples at maximum temperatures of 213 K and 193 K, respectively. Retention of diffusible elements can now be increased by optimizing the freeze-substitution technique and by using these new resins for cryoembedding. Serial sections of samples prepared by the three cryomethods mentioned above can be used to obtain elemental composition, molecular composition and ultrastructural information (Quintana, 1994).

In spite of these good characteristics such cryomethods are little used because technical difficulties are still encountered. The most important is working at low temperatures and maintaining samples at this temperature throughout the whole processing, including polymerization. Lowicryl resins are also toxic (Tobler and Freiburghaus, 1990) and many workers have become sensitized.

In the last few years (1989-1992) we have focused our activity mainly on building low-cost, safe devices for cryofixation, freeze-substitution and cryoembedding that provide reproducible results. We have constructed a system for cryofixation by quick immersion in liquid propane, a system for cryoembedding and a system for

combined freeze-substitution and cryoembedding.

The main goal of this paper was to compare the results obtained with our home-made devices. Another aim was to demonstrate some new possibilities concerning the processing of microanalytical data recorded with these devices (spectra and X-ray maps). In recent papers (Quintana and Ollacarizqueta, 1989; Quintana, 1991a) we have described possible applications of multivariate statistical analysis (MSA) with data obtained after processing X-ray data. It was also demonstrated that MSA can be applied directly to series of spectra (Bonnet *et al.*, 1991; Bonnet and Trebbia, 1992) or images (Hannequin and Bonnet, 1988; Trebbia and Bonnet, 1990; King *et al.*, 1989; Paque *et al.*, 1990; Bonnet *et al.*, 1992). In this paper, X-ray data obtained on K11M and HM23 Lowicryl cryoembedded quail and liver tissues were analyzed with the help of MSA. It is shown that this method provides useful tools for interpreting more objectively a complex data set and for establishing the relationship between the diffusible elements and the P and S elements in different cellular areas.

Materials and Methods

Cryosystems

We have built systems for: cryofixation by rapid immersion in liquid propane, cryoembedding in K11M Lowicryl resin and combined freeze-substitution and cryoembedding in K11M or HM23 Lowicryl resins.

The details of these cryosystems have been described previously (Halpern and Quintana, 1989; Quintana, 1991a,b; 1994). A brief explanation is given below:

System for cryofixation by quick immersion in liquid propane. The basic equipment and the cooling principles are:

[1] The system uses commercial propane with a melting point lower than that of pure propane. Thus, it remains liquid at the boiling point of liquid nitrogen (77K) and it is not necessary to use any temperature regulation system.

[2] The system is equipped with a spring assisted injector based on the Robards and Crosby (1983) device (in Robards and Sleytr, 1985). The kinetic energy required to rapidly plunge the specimen into the propane is supplied by the compression of a spring. A second spring acts as shock absorber. In this system a turbulent flow around the specimen is created that increases the heat transferred between the surface of the sample and the cryogenic liquid. The system is very simple, quick to start off and it can be transported out of the laboratory (operation theater, field studies, etc.) because it does not require any energy source. With this system it is possible to preserve the morphology up to several tens of micrometers from the freezing edge.

System for cryoembedding. We have modified and adapted a Pasteur-Institute device for progressive lowering of temperature (PLT) dehydration and Lowicryl K4M infiltration existing in our laboratory.

The basic equipment and the cooling principles are:

[1] An insulated work chamber (polyester box) cooled by liquid nitrogen (LN_2).

[2] A constant shaking of the specimen during the resin infiltration process.

[3] Polymerization in open flat embedding moulds. In these moulds (of small dimension) it is possible to orient the samples and the heat of polymerization of the resin is more efficiently removed.

With this device it is possible to maintain a temperature of 213K with a nitrogen supply of 0.3 l/h.

System for freeze-substitution and cryoembedding. This system was developed in 1991 (Quintana, 1991b). Some modifications were subsequently proposed (Quintana, 1992).

The main characteristics are:

[1] The cold source is a commercial freezer with a minimum temperature of 180K.

[2] The freezer contains a set of work modules: [a] a new shaking device, consisting of a platform that swings on a fixed framework; a methacrylate carrier tray is mounted on this platform; the organic medium container is placed on it. The platform is made to swing by the movement of a permanent magnet between opposing coaxial magnetic fields from two coils attached to the framework. An external electronic circuit allows the regulation of the intensity of the current and the periodicity of the swinging movement, [b] a stainless-steel platform with room for a specimen holder and two flat embedding moulds, [c] a stainless-steel box for cryopolymerization. During the polymerization a variable flow of cooled dry nitrogen gas flows above the moulds.

[3] After cryofixation, the samples remain in a single specimen holder during the FS and cryoinfiltration processes. The jars containing the organic substituting and infiltrant media are closed.

[4] The temperatures of the organic media and the embedded samples are measured with a Pt-100 thermoresistor.

[5] The samples are manipulated between the different work modules under a continuous flow of cooled dry nitrogen gas, into a plastic chamber placed on the freezer that is equipped with two diaphragms for introducing the hands.

In this device manipulation is very quick, easy and completely safe.

Table 1. Characteristics of the analytical electron microscopes used.

	TEM/STEM Hitachi 800	*TEM JEM 2000FX*	*TEM/STEM Philips CM20*
Voltage (kV)	200	200	200
electron source	tungsten	tungsten	LaB_6
d_s(nm)	20-400	100-400	14-19
cold stage	no	no	yes (113K)
EDS	Quantum UTW	Link UTW	Quantum UTW
X-ray detector	10 mm^2 $\alpha=0°$ $\beta=68°$ $\gamma=0.011$	10 mm^2 $\alpha=0°$ $\beta=70°$ $\gamma=0.020$	30 mm^2 $\alpha=90°$ $\beta=40°$ $\gamma=0.16$
X-ray analyzer	Microanalyst Kevex 8000	AN10000 Link	AN10000 Link

α=azimuth angle, β= take-off angle, γ= solid angle, d_s= diameter of the probe.

Sample preparation

Cryoembedding in K11M. In the first series of experiments fragments of quail oviduct and liver tissues were prepared by the following procedure: Fragments of several mm^3 of anaesthetized rat or decapitated laying quail were cut and immersed in a culture medium (Sigma M 7653). Smaller fragments of about $1mm^3$ were then progressively cut and cryofixed in a commercial Cryovacublock system (Cambridge Instruments, UK).

After cryofixation, the samples were freeze-substituted in pure acetone in a commercial Cryocool system (RUA Instruments, Paris, France) at 183K for 3 days. After that, the samples were transferred to the home-made cryoembedding device described above. In this system the freeze-substituted samples were successively placed in glass tubes containing the precooled cryoinfiltration mixtures. The infiltration protocol was :

- resin-acetone 1:1 for 4h at 213K
- resin-acetone 2:1 for 4h at 213K
- Pure resin for 4h at 213K
- Pure resin overnight at 213K

Cryopolymerization was carried out in open flat embedding moulds under UV and an inert nitrogen (N_2) atmosphere for 4 days at 213K and 2 days at room temperature.

Cryoembedding in HM23. In a second series of experiments fragments of onion root and liver tissues were prepared by the following procedure: [1] small fragments of about 1 mm^3 of onion root were progressively cut and rapidly cryofixed by quick immersion in liquid propane in our home-made device, [2] small fragments of about $1mm^3$ of liver tissue were progressively cut from an anaesthetized rat and immediately cryofixed by quick immersion in liquid propane in our home-made device.

After cryofixation, the samples were transferred into the single specimen holder placed in the cryofixation system. After that, the single specimen holder was transferred to the home-made cryosystem for freeze-substitution and cryoembedding described above and successively immersed in glass jars containing the precooled pure acetone (183K) and cryoinfiltration mixtures of HM23 resin and acetone. The protocol for freeze-substitution and cryoinfiltration was similar to that previously described for K11M except that the work temperature in this case was 193K. The single specimen holder was transferred to work module number two and the samples placed in the small open moulds. During the polymerization the temperature was continuously registered. The flow of cooled dry nitrogen flowing above the moulds was regulated so that the sample temperature was maintained close to 193K.

X-ray microanalysis

For X-ray microanalysis dry-cut sections of about one micrometer thick were obtained using glass knives

Table 2. X-ray mapping conditions.

	TEM/STEM Philips CM20
pixels	128*128
time/pixel	10ms
number of frames	8-14

and spread directly on Ti or Ni grids.

Energy-dispersive X-ray spectra (EDS) and X-ray maps were recorded at 200kV in different analytical electron microscopes. The characteristics of these instruments are summarized in Table 1.

Treatment of individual X-ray spectra. The X-ray spectra were treated in the following way:

[1] Subtraction of continuum X-ray background by using a model based on Kramer's law (Microanalyst Kevex 8000 system) or by a least-squares fit to filtered profiles method (Link AN10000 system).

[2] Deconvolution of the Kα line from Ca and the Kβ line from K with a Gaussian method (Microanalyst 8000 Kevex system) or with the least-squares fit to filtered profiles method (Link AN10000 system).

[3] Semi-quantitative analysis by the Cliff-Lorimer standardless method (Cliff and Lorimer, 1975).

The Lowicryl resins have a density close to one. Therefore, in embedded Lowicryl samples (Hall, 1991) the measured concentrations are a good estimation of the wet mass fraction (Quintana and Bonnet, 1994) if we assume that

$$\Sigma(\text{Na, Mg, P, S, Cl, K and Ca}) = 0.01 \qquad (1)$$

X-ray mapping. X-ray mapping of C, O, P, S, K and continuum X-rays were carried out with a Philips CM20 transmission electron microscope/scanning transmission electron microscope (TEM/STEM). The mapping conditions are given in Table 2.

Processing of individual images

The imaging techniques used in this study are close to the limits attainable by state-of-the-art technology. Thus, images are not of very good quality, compared to images obtained with more classical imaging devices:

- X-ray maps are very noisy, due to the small amount of counts allowed by the acquisition time, which is necessarily limited

- TEM/STEM bright field images have low contrast, due to the absence of chemical staining

Therefore, these images have to be processed in order to be displayed or to allow any kind of quantification.

There are a lot of available procedures for contrast enhancement or improvement of the signal-to-noise ratio (S/N). However, these procedures are not entirely suitable for this kind of image. For instance, image smoothing (intended to improve S/N) also degrades the resolution. Therefore, new methods (called locally adaptive methods) were used for the improvement of S/N and for contrast enhancement. For more details on these methods see Quintana and Bonnet (1994) and Vautrot *et al.* (in preparation).

Multivariate statistical analysis

Multivariate statistical analysis (MSA) is the generic term used to designate a group of methods able to extract the significant information contained in complex data sets (Benzecri, 1978; Lebart *et al.*, 1979; Foucard, 1982). The data set is supposed to be a table of n individuals and N quantitative variables (characters). Different normalization procedures of the original data set lead to different variants of MSA [e.g., principal component analysis (PCA); Karhunen-Loeve analysis (KLA); factorial analysis of correspondence (FAC)].

The principle of the technique is to transform the N original characters, which are more or less correlated, into M new characters, which are uncorrelated. The solution is found for the linear combination of the N original variables which maximizes the variance of the individuals. These new axes (principal or factorial axes) define a new (orthogonal) multidimensional space which is better adapted to the data set. It is then possible to compute:

- the coordinates of the individuals in this new representation.

- the coordinates of the initial variables on these new axes (rotation angles).

From these two sets of coordinates, it is possible to deduce the correlation between individuals (which can be gathered into several groups), between variables and between variables and individuals.

The visualization of these two sets of coordinates allows also an interpretation of the principal axes to be derived and thus of the information contained in the original data set.

Analysis of data sets deduced from X-Ray spectra. The processing of one spectrum provides the concentration of several elements. When several spectra are recorded at different places in equivalent biological compartments, some kind of averaging can be performed and the interpretation of the results is relatively straightforward. But when many spectra are recorded within several different regions of interest, the data set becomes

more complex and more difficult to interpret objectively. This interpretation can be made easier by applying MSA, with the different elements as variables and the position of the analysis as individuals.

PCA was used and performed with the STATITCF software on a Personal Computer (PC). The results (coordinates of variables and individuals on the principal axes) are displayed as graphs onto principal planes (axes 1-2, 1-3, 2-3, etc.). On these graphs, similarities and differences between variables (or individuals) can be appreciated through the proximity or remoteness of their projections.

Analysis of series of X-ray maps. A series of N images (e.g., X-ray maps of N elements) constitutes a data set in a N-dimensional space. One method for analysis of such a large data set consists of finding a reduced M-dimensional space (M < N) where it may be more easily interpreted. In practice, this means that one would like to get:

- an overview of the correlations and anticorrelations existing between the different elements
- a reduction of the set of N images (X-ray maps) into a smaller set of M images which display regions of the images where most of the information is concentrated.

This is exactly what can be done by one of the variants of MSA (e.g., PCA, FAC, KLA). The only difference compared to such an analysis applied to simple results of measurements is that the number of individuals, n, is greater (16384 for 128*128 pixels maps). Otherwise, the steps of the analysis are similar:

[1] Build a matrix with the normalized experimental data: Y(i,j)

j = X-ray map number

i = pixel number

Y = number of counts for pixel i of map j

[2] Build the variance-covariance matrix

$S = Y^t.Y$

t means the transposed matrix

[3] Perform the eigenvalue-eigenvector decomposition of the variance-covariance matrix.

The first eigenvectors thus form a new orthogonal basis for the representation of the data set. In this work, we have mainly used factorial analysis of correspondence (FAC) as a variant of MSA, but similar results can be obtained with other variants (e.g., PCA or KLA). It is only when quantitative results are expected that the method for data normalization has to be selected carefully. The X-ray pixel maps may then be represented by their coordinates on the different axes (eigenvectors), and mapping these coordinates on the plane defined by two of these axes helps to visualize the correlation or anticorrelation between the different elements. When these coordinates are converted into grey levels, they may be displayed as factorial images. One may then visualize regions of the object which are responsible for the main sources of information in the original data set.

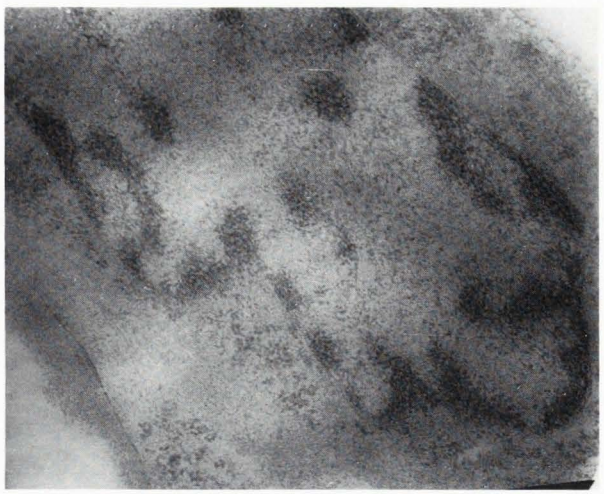

Figure 1: Quail oviduct. Stained section of cryofixed (CF) freeze-substituted (FS) and K11M Lowicryl cryoembedded (CE) tissue. Detail of a nucleus. Ice crystals are not visible. Bar = 1 μm.

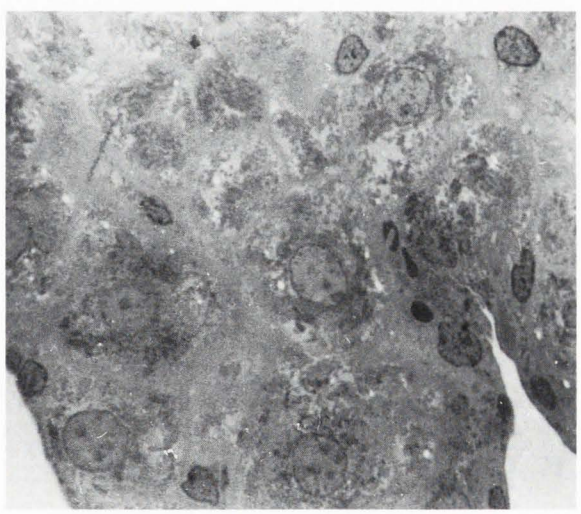

Figure 2: Rat liver. Stained section of CF, FS and MH23 Lowicryl CE tissue. Bar = 10 μm.

Results

Ultrastructure

Quail oviduct cryoembedded in K11M. After cryofixation, freeze-substitution in pure acetone and cryoembedding in Lowicryl K11M, the morphology of

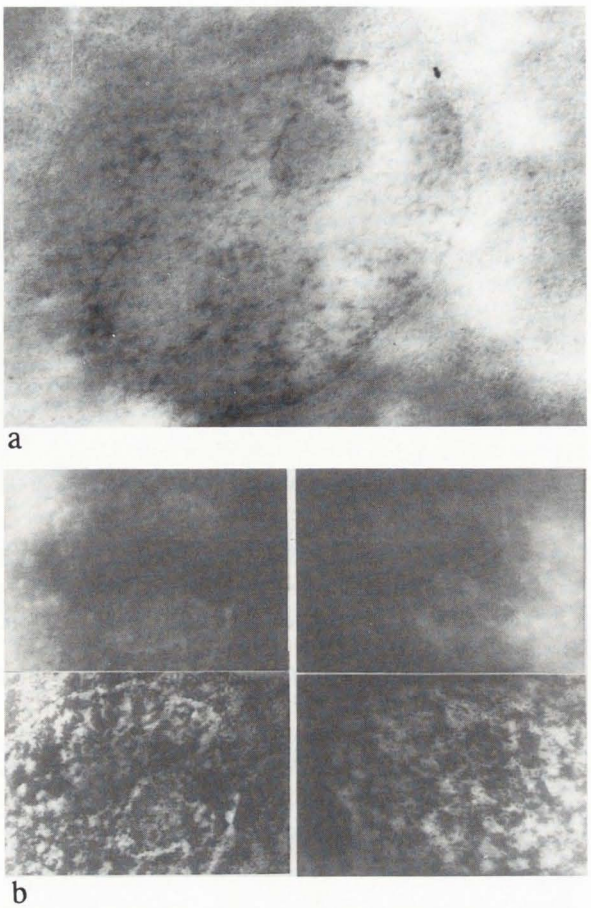

Figure 3: Rat liver. Unstained dry-cut section of CF, FS and MH23 Lowicryl CE tissue. (a) The contrast has been increased by the photographic process. Bar = 1 μm. (b) Digitalized images before and after local digital filtered process. Bar = 1 μm.

the epithelium and the tubular gland cells next to the epithelium was found satisfactory for immunocytochemical studies (Quintana *et al.*, 1991). All the cellular organelles can be recognized and the mucus granules have the same morphology as found in tissues that were cryofixed, freeze-substituted in acetone plus osmium tetroxide, and embedded at high temperature in Epon (Sandoz *et al.*, 1985). Some nuclei are free of ice crystal damage (Fig. 1) and the cell membranes are often visible.

Liver tissue cryoembedded in HM23. In accordance with our recent description (Quintana 1993, 1994) the ultrastructure was found to be satisfactory over 2 or 3 cell layers at the surface of cryofixed liver fragments (Fig. 2). Ice crystals were not observed in those nuclei located near the cryofixation front. Fig. 3 shows examples of nucleus images obtained from unstained sections of about one micrometer thick. The contrast is weak but it is possible to identify the condensed chromatin, the nucleolus and the nucleoplasm. Local contrast enhancement of images allows a better visualization of these structures (Fig. 3).

X-ray microanalysis

Quail oviduct cells cryoembedded in K11M. X-ray analysis was performed on dry-cut sections of quail oviduct spread on the Ti grid without any solvent. In all the cells analyzed we observed the presence of the diffusible elements Na, Mg, Cl, K and Ca and the elements P, S, Cu and Zn at different concentrations. Metals such as Fe, and Co originating from the specimen chamber are often detected and should be considered as artefacts. Characteristic X-ray spectra of chromatin and cytoplasmic areas are shown in Fig. 4.

Onion root and liver cells cryoembedding in HM23. X-ray analysis of several cytoplasm and nucleus areas of onion root and liver tissues are shown in Fig. 5 and Fig. 6.

The K/Na ratio in intact cells (K/Na between 8 and 24 in onion cells and K/Na between 3 and 12 in liver cells) is in the order of physiological values (Cameron *et al.*, 1984; Somlyo *et al* ., 1985; Von Zglinicki and Bimmler, 1987; Zierold, 1988).

MSA applied to a set of spectra

Quail oviduct cells cryoembedded in K11M. MSA was applied to a set of 35 measurements on different nuclear and cytoplasmic areas. The correlations between the variables (elements) and the individuals on principal axes are shown in Table 3 and Fig. 7.

We observe :

- correlation between P and Mg in axis 1,
- strong correlation between S, Cl, and K in axis 1,
- correlation between Na, Mg, K, and Ca in axis 2.

Axis 1 represents the opposition between P (Mg) and the group of elements S, Cl, K and Ca. Axis 2 represents the opposition between the S and Cl and the group Na, Mg, K and Ca.

The analyzed areas may be divided, in plane 1-2, into three groups G1, G2 and G3. G1 is formed by the measurements over the nuclei (●) and groups G2 and G3 (▲ ★ ■) are formed by the measurements on the cytoplasm of cells, mucus granules and secretion granules. The mean values for the concentrations in each group are shown in Table 4. The strong anticorrelation between P(Mg) and the group (S, Cl and K) separates the nuclear areas and the cytoplasmic areas. The nuclei have a higher P (and Mg) concentration and a lower S, Cl and K concentration than the cytoplasm. Groups G2 and G3 contain the mucus granules (★) and the secretion granules (■) respectively. These groups are separated by axis 2 according to their different S and Cl concen-

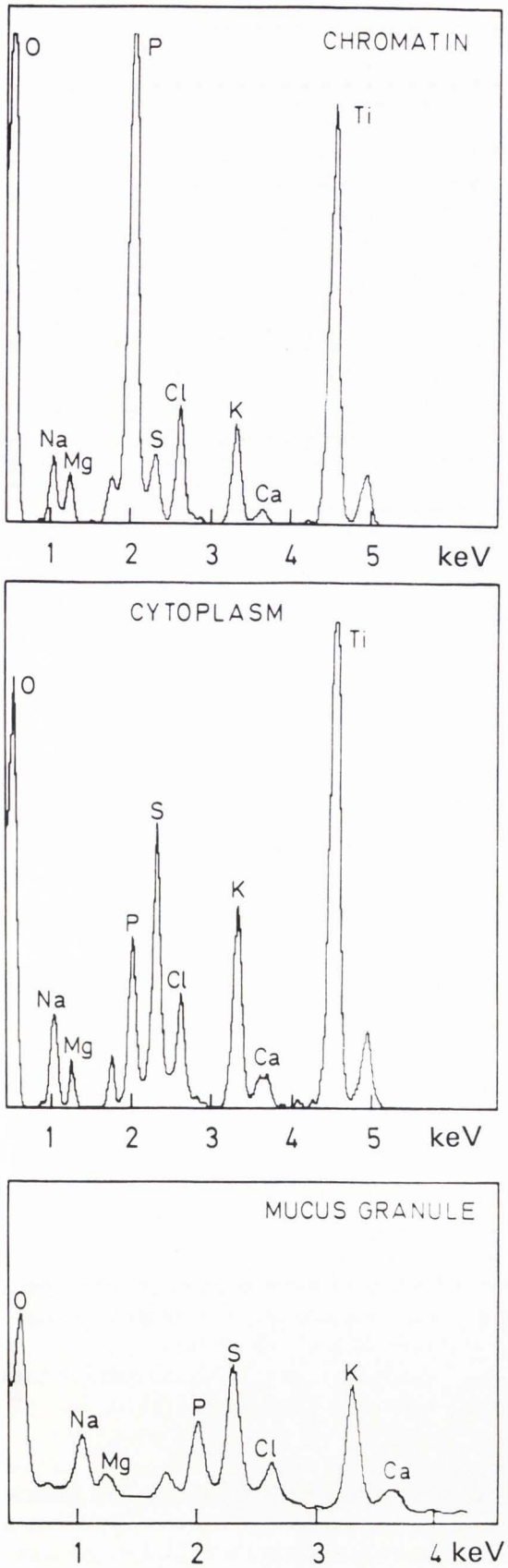

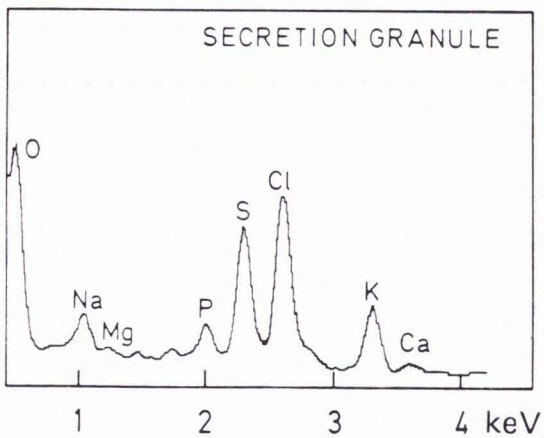

Figure 4: X-ray spectra of different areas of quail oviduct cells after CF, FS and K11M Lowicryl CE. (a) condensed chromatin, (b) cytoplasm, (c) mucus granule, (d) secretion granules. The (a) and (b) spectra are continuum background substracted. (Hitachi 800MT plus Kevex system)

tration which is higher in secretion granules (Fig. 4c,d).

Liver cells cryoembedded in HM23. MSA was applied to a set of 82 nuclear and cytoplasmic areas of liver cells. Results are shown in Table 5 and Fig. 8.

We observe as before :

- correlation between P and Mg in axis 1
- correlation between S, Cl and K (Ca) in axis 1
- anticorrelation between the group (P, Mg) and the group (S, Cl and K) in axis 1.

and in addition:

- correlation between K and P in axis 2
- anticorrelation between K (and P) and the group Na, Mg and Ca (and S) in axis 2.

Axis 1 represents, as before, the opposition between (P, Mg) and (S, Cl, K and Ca). Axis 2 represents the opposition between (K, P) and (Na, Mg, Cl, Ca and S).

As before, the strong anticorrelation between P (Mg) and S (Cl and K) separates the nuclear areas (■ □ ▵) and the cytoplasmic areas (★); the nuclei have a higher P concentration and a lower S, Cl and K concentration.

Three different groups may be distinguished in relation to plane (1-2). Group G1 is formed by those areas identified as nucleolus or condensed chromatin, group G2 is formed by the cytoplasmic areas and group G3 an intermediary, is formed by measurements in the nucleoplasm and in the cytoplasm close to the nuclei. Table 6 shows the mean values for the concentrations in groups G1, G2 and G3. The measurements in group G3 taken inside and outside the nuclei have been grouped

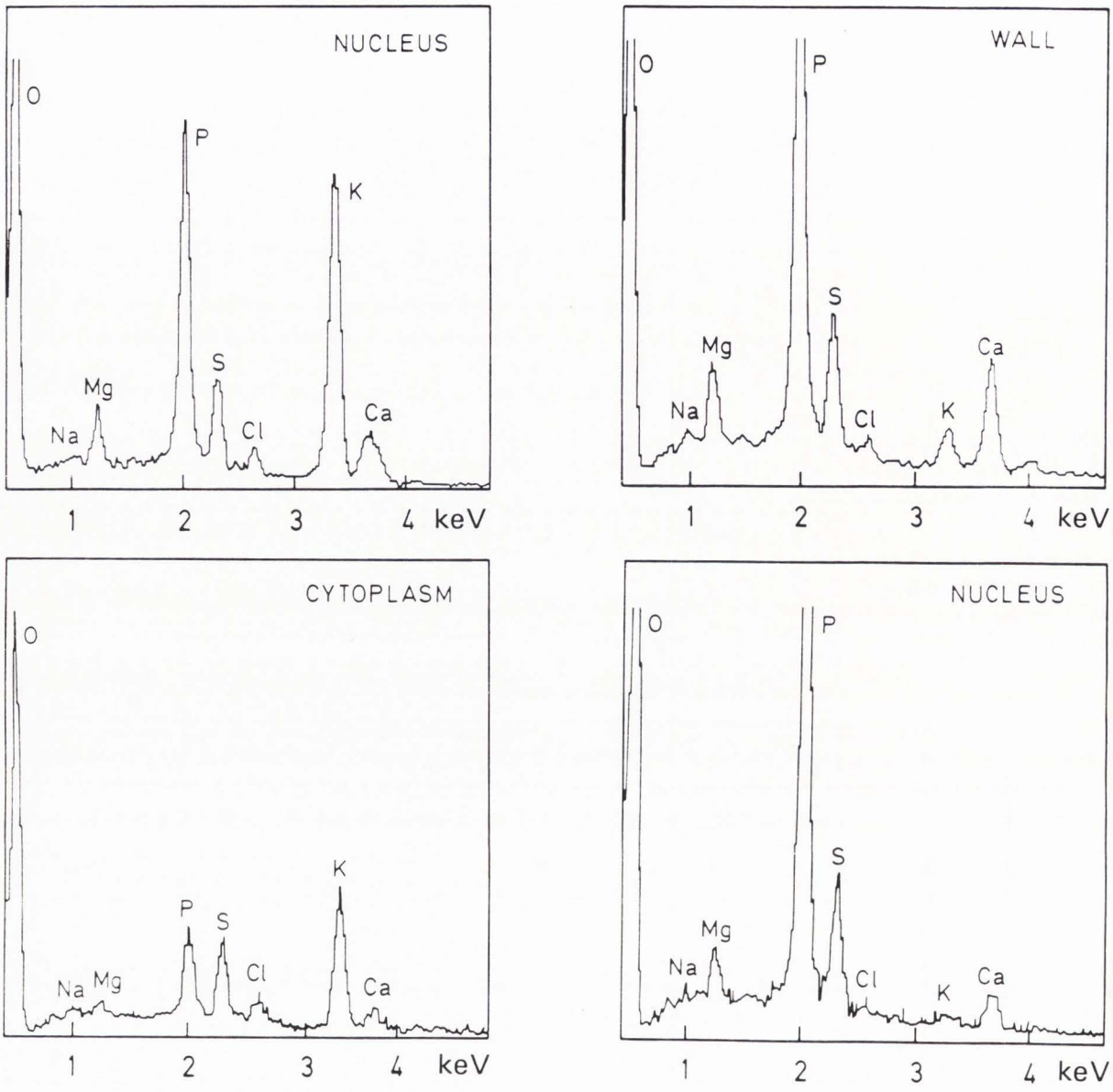

Figure 5: X-ray spectra of different areas of onion root cells after CF, FS and HM23 Lowicryl CE. (a) nucleus. (b) cytoplasm. (c) wall of well preserved cell. (d) nucleus of poorly preserved cells. (JEM 2000FX plus Link system).

together as there is no significant difference between them. Axis 2 differentiates measurements over different nuclei (see Quintana and Bonnet, 1994) according to the difference in K concentration.

X-ray maps

Liver cells cryoembedded in HM23. X-ray images for those elements with the highest concentration (O, P, K, and S) and for the X-ray continuum image (CB) were recorded (Fig. 9 and 10). The X-ray continuum image reveals the mass-thickness effect (ρt) which has a very small variation among the different areas displayed in case of absence of heavy elements.

Table 7 shows the number of counts obtained from the set of X-ray images displayed in Fig. 10.

MSA applied to X-ray maps

Liver cells cryoembedded in HM23. The factorial analysis of correspondence (FAC) was applied to a series of 4 characteristic images (recorded images minus

Table 3. ACP analysis.

	Axis 1 (34.1%)	Axis 2 (27.8%)	Axis 3 (13.7%)
Na	-.0213	.5363	.7567
Mg	.2001	.7339	-.1366
P	.9655	-.0801	-.0324
S	-.8140	-.2749	.-1223
Cl	-.6151	-.3966	.3825
K	-.5453	.6062	-.4391
Ca	-.2724	.7167	.1062

Correlation between the variables and the principal axis. The contribution to the total variance from each axis is indicated in brackets.

continuum image) from O, P, S and K (Tables 8 and 9). The results over areas including one nucleus with surrounding cytoplasm acquired at a magnification of 20,000 are shown in Fig. 10. The nuclear areas which include the nucleolus were also acquired at a higher magnification (X 30,000). (Fig. 11).

As in PCA of a set of nuclei spectra, axis 1 represents the opposition between the group of elements (K and P) and the element S, and axis 2 represents the opposition between the group (K and S) and the element P.

The factorial images over axis 1 (F1) show how the P and K correlation differentiates those areas which contain nucleic acids from the nucleoplasm and cytoplasm. The factorial images over axis 2 (F2) show how the S and K correlation differentiates the protein-containing areas in the nucleus and in cytoplasm from the regions containing high nucleic acid concentrations.

Discussion

Under physiological conditions the intracellular K/Na ratio is greater than 5. In the quail oviduct cryoembedded in Lowicryl K11M (at 231 K) the K/Na ratio is close to one (with Na concentrations higher and K concentration lower than the physiological concentrations). Therefore, the elemental balance between the K and the Na seems disturbed. The redistribution of diffusible elements may take place at two different moments: [1] Before cryofixation, i.e., during sampling, [2] During the FS and LTE processes.

In this set of experiments we have used the Cryovacublock as the cryofixation system. We kept the dissected fragments of liver and the quail oviduct in a culture medium (M 7653, Sigma) for several minutes

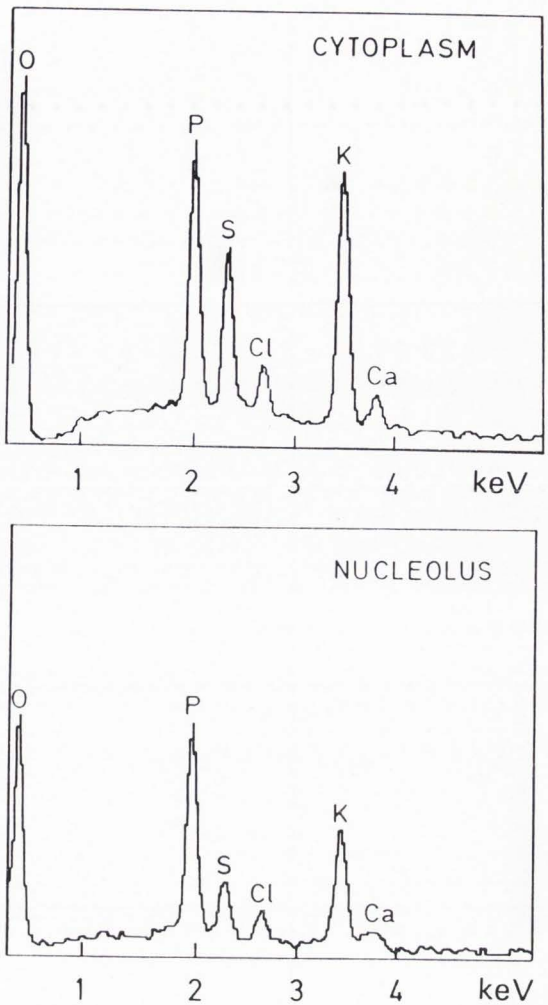

Figure 6: X-ray spectra of different areas of rat liver cells after CF, FS and HM23 Lowicryl CE. (a) cytoplasm (b) nucleolus. (JEM 2000FX plus Link system)

before cryofixation. In this medium the ciliary movement of epithelial oviduct cells is maintained for several hours. Moreover, as in Ringer's solution, a redistribution between the intra-extra cellular medium is possible.

Our X-ray data on the liver tissues are similar to those obtained by Zierold (1988) on freeze-dried cryosections of excised liver tissues (Quintana, 1994). In both cases, independently of cryomethods used, the K/Na ratio is smaller than that obtained by Zierold himself on cultured liver cells after FD/CS.

In muscle cells, Edelmann (1991) has shown that 70% of K can be retained on K11M CE samples, in comparison with FD/CS samples.

Therefore, the intracellular loss of K and increase of Na (and Ca) in this first set of experiments are more probably due to an incorrect sampling than to a possible redistribution of these elements during the FS and/or

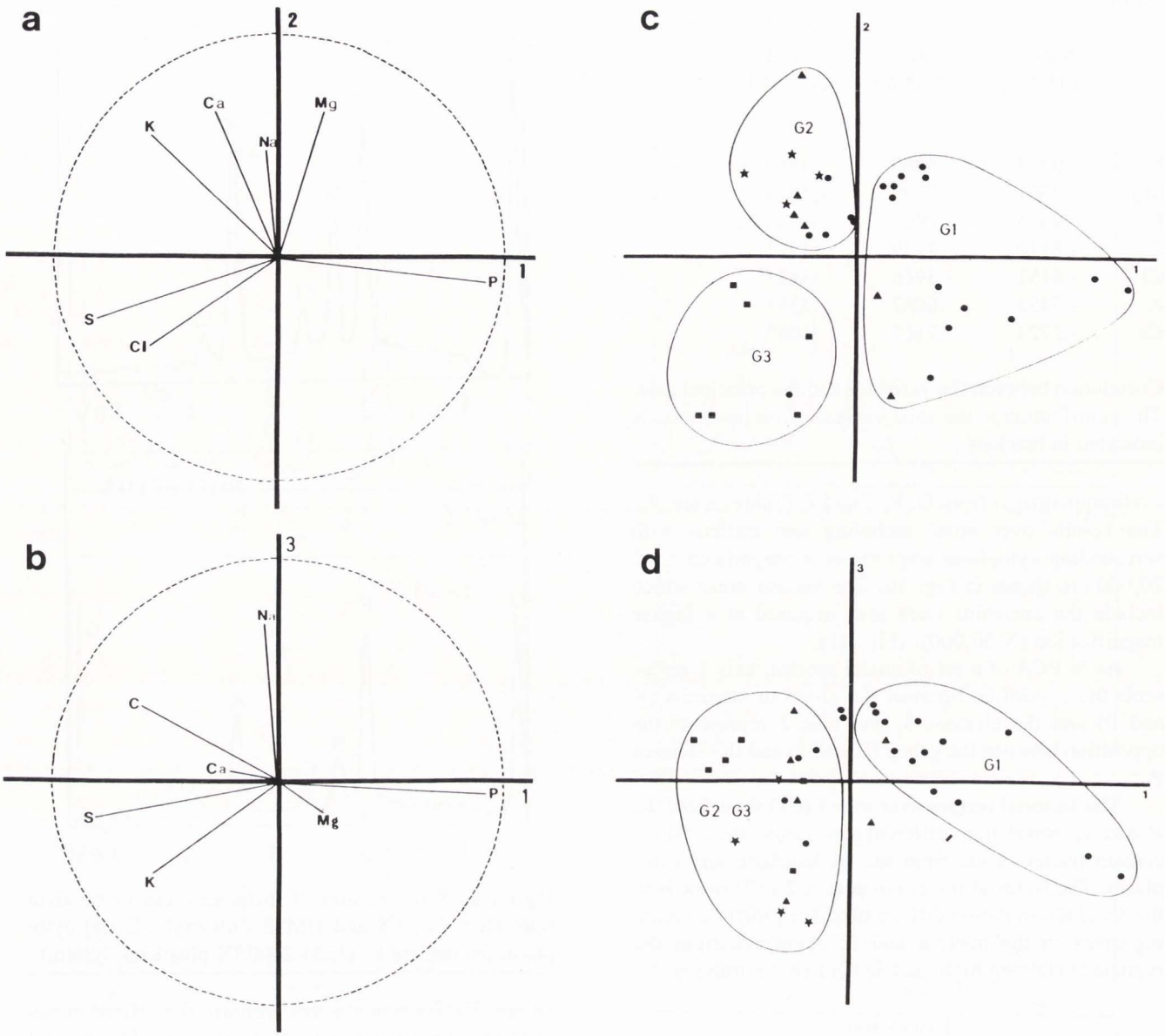

Figure 7: Quail oviduct after CF, FS and K11M Lowicryl CE. Multivariate statistical analysis (MSA) of a set of 35 measurements over different nuclear and cytoplasmic areas. (a, b) variable analysis. (c, d) individual analysis.

CE. To prove that this hypothesis is right it was necessary to improve: [1] the preparative protocol prior to cryofixation, [2] the CE protocol by using even lower temperatures.

In onion root and liver cells cryofixed by fast immersion in liquid propane, freeze-substituted in pure acetone (at 183K) and cryoembedded in Lowicryl HM23 (at 193K) the conditions mentioned above are accomplished. The K/Na (and the K and Na concentrations) obtained in these tissues correspond to physiological conditions.

MSA applied to a set of spectra and X-ray maps allowed us to show that:

- the cytoplasm and the nuclei form two different compartments which differ by their concentrations of P and S. This is independent of the partial loss of K and increase of Na, Mg and Ca due to sampling or redistribution during the preparative processing.
- Mg is correlated with P in the nucleus
- there is a strong correlation between S and Cl
- there is a high affinity of K with P in nucleic acids and with S in proteins (cytoplasmic and nuclear).

Factorial images constructed from MSA of X-ray maps, allow the specific visualization of the areas of correlation

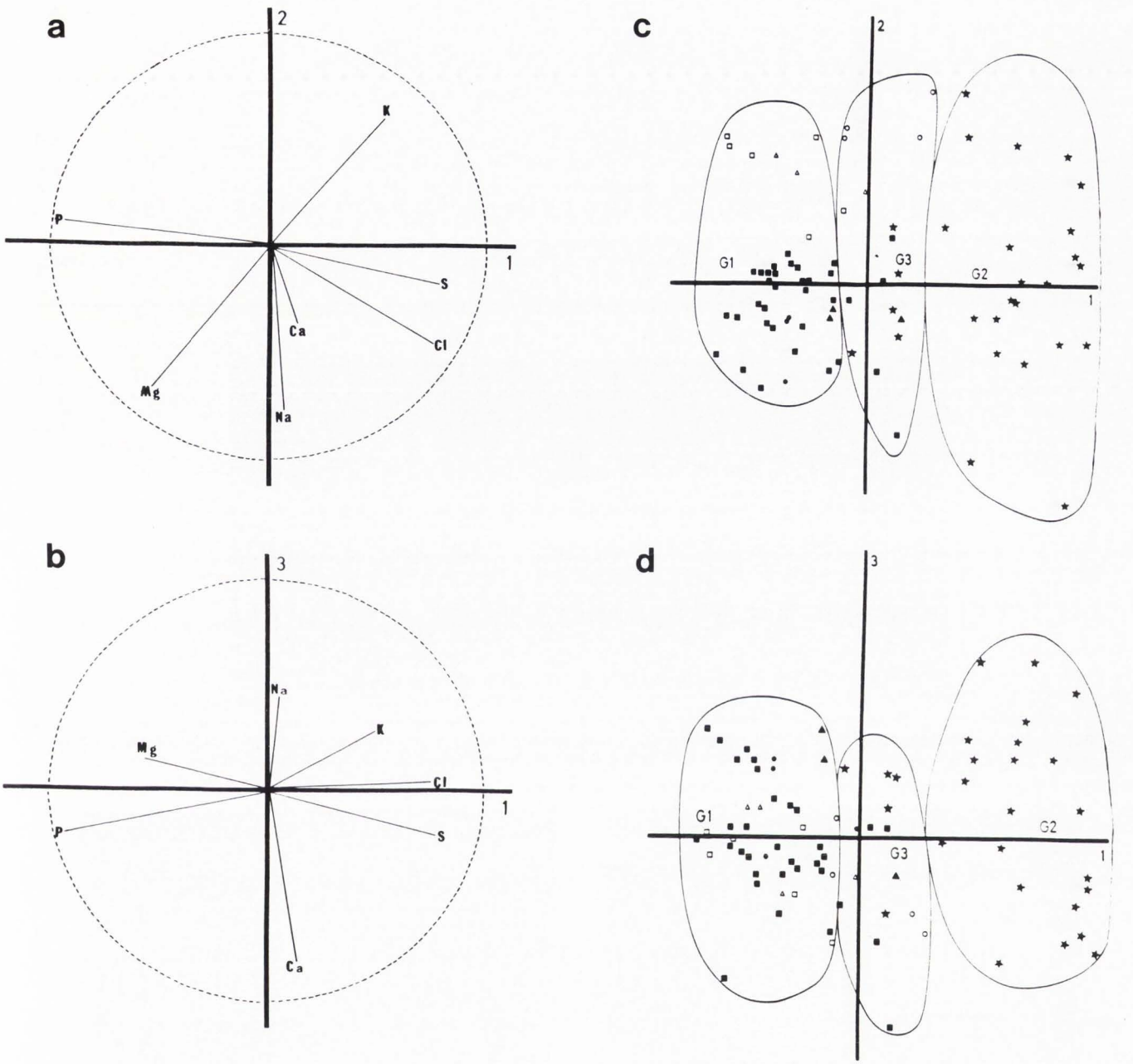

Figure 8: Rat liver after CF, FS and HM23 Lowicryl CE. Multivariate statistical analysis (MSA) of a set of 82 measurements over different nuclear and cytoplasmic areas. (a, b) variable analysis. (c, d) individual analysis.

between K and P (the nucleic acids) and between K and S (the cytoplasmic and nuclear proteins). This supports the hypothesis that K is linked to phosphate groups in nucleic acids and anionic groups of amino acids (Negendank, 1989; Cameron *et al.*, 1990; Warley, 1992).

MSA made it possible to go from a chemical distribution (elements O, P, S and K) toward a molecular interpretation (in terms of nucleic acids and proteins).

Conclusion

Cryofixation, freeze-substitution in pure acetone at

Table 4. Evaluation of the wet mass fractions

	Na	Mg	P	S	Cl	K	Ca
G1 Nuc (n=19)	16±1	4±0.4	32±3	15±1	18±1	13±1	2±0.3
G2 Cyt+muc (n=10)	14±4	4±2	19±7	24±4	17±5	19±6	4±2
G3 Secr gran (n=6)	11±4	2±1	11±5	30±6	29±5	15±3	1±0.8

Concentration mean values ($*10^4$) (± standard deviation of the mean) in the groups. Nuc = nuclei, Cyt = cytoplasm, muc = mucus cell, secr gran = secretion granules.

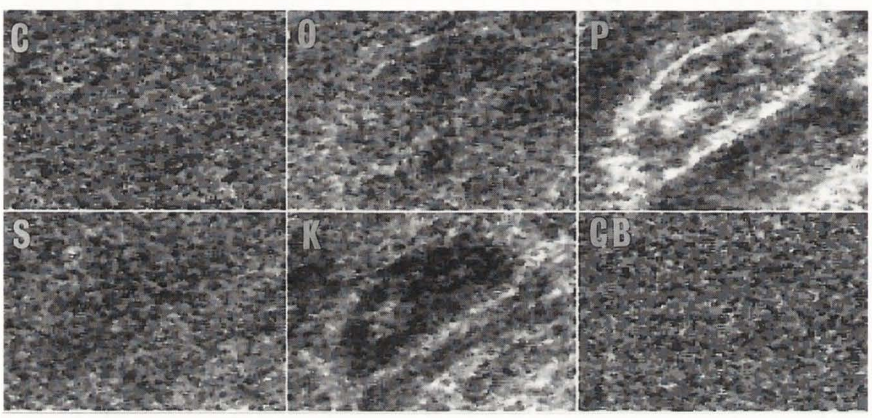

Figure 9: Set of X-Ray maps of C, O, P, S and K and continuum X-Ray (CB) image of a liver cell after CF, FS and HM23 Lowicryl CE. Bar = 5 μm.

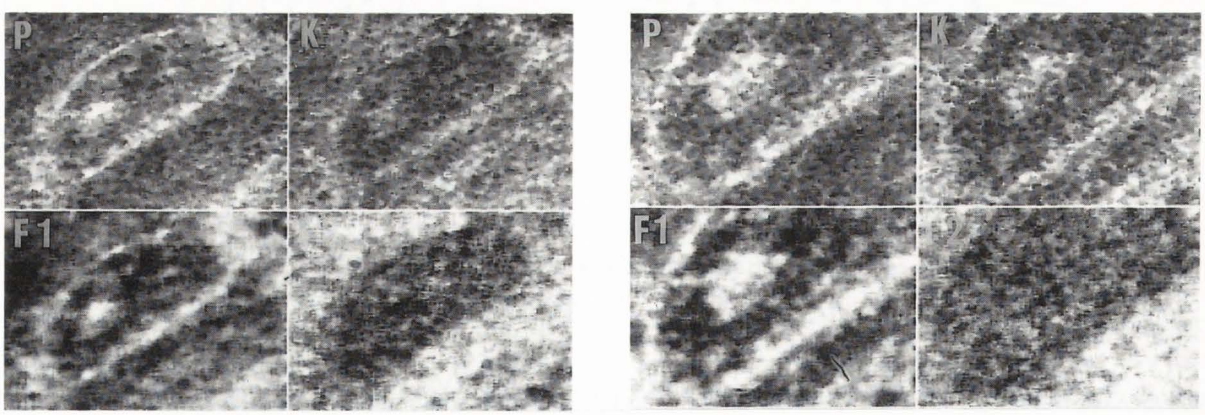

Figure 10: (a) Set of X-Ray maps of P, K and factorial images on axis 1 (F1) and axis 2 (F2). (b) Idem over a part of the nucleus acquired at higher magnification. Bar = 2 μm.

183K and cryoembedding in HM23 resin at 193K are a set of cryomethods allowing the preservation of diffusible elements at subcellular level similar to the preservation obtained with the FD/CS methods.

In embedded tissues the elements are diluted about a factor of 3 compared with the concentration obtained in freeze-dried cryosections. In Lowicryl resins the measured concentrations are close to the concentrations in hydrated tissues because their density is close to the density of water. In spite of their low concentration, X-

Table 5. PCA Analysis.

	Axis 1 (41.1 %)	Axis 2 (25.1%)	Axis 3 (15.2%)
Na	.0425	-.7648	.4538
Mg	-.5601	-.6474	.1814
P	-.9506	.1655	-.1833
S	.8377	-.1535	-.1899
Cl	.8030	-.4268	.0110
K	.5432	.6290	.2944
Ca	.1240	-.3485	-.8183

Correlation between the variables and the principal axis. The contribution to the total variance from each axis is indicated in brackets (82 points analyzed: set of 5 nuclei and cytoplasm).

ray maps of P, S, K and O can be obtained with a signal-to-noise adequate for image interpretation.

MSA methods applied to X-ray spectra and X-ray maps constituted a powerful tool for the analysis of the relationship between the diffusible and non diffusible elements at subcellular level. MSA could be also applied to simultaneously acquired X-ray (P, S, K and O) and PEELS (O, N, Na, Mg and Ca) data (Leapman and Hunt, 1991) on the same areas. This will provide greater knowledge of the physio-pathological compartmentation of diffusible elements at subcellular level.

Acknowledgements

The authors wish to thank Dr. Duval and Dr. Lemarchand from the Electron Microscope Service of Rouen University (France) for the technical support and Dr. Boulanger from C.E. Saclay/DTA/CEREM/SRMP (France) for giving us access to AEM Philips CM20 and for helpful discussions. This work was partially supported by the Mercure French Spanish Programme (Barcelona University, Spain)

References

Benzecri JP (1978) *L'analyse des Données (Analysis of Data)*. Dunod, Paris.

Bonnet N, Trebbia P (1992) Multi-dimensional data analysis and processing in electron-induced microanalysis. Scanning Microsc Suppl **6**: 163-177.

Bonnet N, Simova E, Thomas X (1991) Application of multivariate statistical analysis to time dependent spectroscopy. Microsc Microanal Microstruct **2**: 129-142.

Bonnet N, Simova E, Lebonvallet S, Kaplan H (1992) New application of multivariate statistical analysis in spectroscopy and microscopy. Ultramicroscopy **40**: 1-11.

Cameron IL, Hunter KE, Smith NK (1984) The subcellular concentration of ions and elements in thin cryosections of onion root meristem cells. J Cell Sci **72**: 295-306.

Cameron IL, Hardman WE, Hunter KE, Haskin C, Smith NKR, Fullerton GD (1990) Evidence that a major portion of cellular potassium is "bound". Scanning Microsc **4**: 89-102.

Cliff G, Lorimer GW (1975) The quantitative analysis of thin specimens. J Microsc **103**: 203-207.

Edelmann L (1991) Freeze-substitution and the preservation of diffusible elements. J Microsc **161**: 217-228.

Foucard T (1982) *Analyse Factorielle: Programmation sur Microordinateur*. (Factorial Analysis: Personal Computer Programming), Masson, Paris.

Hall TA (1991) Suggestions for the quantitative X-ray microanalysis of thin sections of frozen-dried and embedded biological tissues. J Microsc **164**: 67-79.

Halpern S, Quintana C (1989) Two simple devices for cryofixation and cryoembedding. Biol Cell **67**: 10a.

Hannequin P, Bonnet N (1988) Application of multivariate statistical analysis to energetic image series. Optik **81**: 6-11.

King P, Browning R, Pianetta P, Lindau I, Keenlyside M, Knapp G (1989) Image processing of multispectra X-ray photoelectron spectroscopy images. J Vac Sci Technol **7**: 3301-3304.

Leapman RS, Hunt JA (1991) Comparison of detection limits for EELS and EDXS. Microsc Microanal Microstruct **2**: 231-244.

Lebart L, Morineau A, Fenelon JP (1979) Traitement des Données Statistiques: Méthodes et Programmes (Treatment of Statistical Data: Methods and Programs). Dunod, Paris.

Negendank W (1989) The physical state of potassium in the human lymphocyte: a review. Scanning Microsc **3**: 865-875.

Paque J, Browning R, King P, Pianetta P (1990) Quantitative information from X-ray images of geological materials. Microbeam Analysis 195-198.

Quintana C (1991a) X-ray microanalysis of cell nuclei. J Electron Microsc Techn **18**: 411-423.

Quintana C (1991b) The use of low temperatures embedding in elemental microanalysis immunocytochemistry and ultrastructural studies. In: *Abstr. Colloque Franco-Iberique Microscopie Electronique*. University of Barcelona, Barcelona (Spain): 58-59.

Quintana C (1992) Development of a new cryosystem of freeze-substitution and cryoembedding for

Table 6. Mean values for the concentration in the groups.

	Na	Mg	P	S	Cl	K	Ca
G1(Nuc) (n=43)	5.7±0.3	2.9±0.1	48.4±0.4	12.9±0.3	7.1±0.2	22.4±0.4	0.5±0.06
G2(Cyt) (n=22)	6.3±0.6	1.8±0.2	28.7±0.7	21.6±0.9	11.6±0.5	29.3±1.3	0.6±0.1
G3 (n=17)	4.8±0.7	2.7±0.3	41.0±0.7	18.1±0.5	9.2±0.4	23.0±1.0	0.8±0.1
G3a(Cyt) (n=8)	5.6±0.4	2.7±0.3	39.6±1.0	18.0±0.8	9.5±0.5	23.0±1.0	0.8±0.2
G3b (Npl) (n=9)	4.0±1.0	2.5±0.5	42.0±1.0	17.6±0.7	9.1±0.7	24.0±1.7	0.8±0.1

Concentration as mean values ($*10^4$) (± standard deviation of the mean) in the groups. N is the number of measurements of each group.
Nuc = nuclei (chromatin and nucleolus); Cyt = cytoplasm; Npl nucleoplasm.

Table 7. Example of the number of counts per pixel obtained from one set of images.

	oxygen	phosphorus	sulfur	potassium
average	23	8.5	6.7	6.7
standard deviation	5	3.7	3.1	3.1
minimum	6	0	0	0
maximum	47	28	21	23

Table 8. Results from FAC.

	Axis 1 (52.3 %)	Axis 2 (30.6%)	Axis 3 (17.0%)
O	-.0766	-.0196	.0299
P	.1968	-.1358	-.0363
S	-.0559	.0913	-.1643
K	.1786	.1807	.0636

Variable analysis. Coordinates of variables on the main factorial axes. The contribution from each axis to the total variance is shown in brackets (16384 points analyzed). Set of images displayed in Figure 9.

Table 9. Results from FAC.

	Axis 1 (55.1 %)	Axis 2 (28.5%)	Axis 3 (16.4%)
O	-.0871	-.0224	.0381
P	.20495	-.1453	-.0627
S	-.0996	.1297	-.1768
K	.2378	.1889	.0727

Variable analysis. Coordinates of the variables on the main factorial axes. The contribution from each axis to the total variance is shown in brackets (16384 points analyzed). Set of images displayed in figure 10 at a higher magnification.

processing biological samples. In: *Electron Microscopy 1992* (Rios A, Arias JM, Megías-Megías L, eds) vol 1, Proc EUREM 92, University of Granada, Granada (Spain), pp 363-364.

Quintana C (1993) *In situ* conservation of diffusible elements in liver cells after cryofixation, cryosubstitution and low temperature embedding at 193 K in HM23 Lowicryl resin. Microsc Res Techn **24**: 103-104.

Quintana C (1994) Cryofixation, cryosubstitution and cryoembeding for ultrastructural, immunocytochemical and microanalytical applications. Micron **25**: 63-99.

Quintana C, Bonnet N (1994) Multivariate statistical analysis (MSA) applied to the X-ray spectra and X-ray mapping of liver cell nuclei. Scanning Microscopy **8**, in press.

Quintana C, Ollacarizqueta A (1989) Multivariate statistical analysis of electron probe microanalytical data on cell nuclear constituents. Ultramicroscopy **28**: 315-319.

Quintana C, Lopez-Iglesias C, Lainé-Delaunay MC

(1991) (3-Cryo)methods cryofixation, cryosubstitution and cryoembedding) for processing of tissues for ultrastructural and immunocytochemical studies. Application to oviduct cells of laying quail. Biol Cell **72**: 167-180.

Sandoz D, Nicolas G, Lainé MC. (1985) Two mucous cell types revisited after quick-freezing and cryosubstitution. Biol Cell 54: 79-88.

Somlyo AP, Bond M, Somlyo AV (1985) Calcium content of mitochondria and endoplasmic reticulum in liver frozen rapidly in vivo. Nature **314**: 622-625.

Tobler M, Freiburghaus AU (1990) Occupational risks of (meth)acrylate compounds in embedding media for electron microscopy. J Microsc **160**: 291-298.

Trebbia P, Bonnet N (1990) EELS elemental mapping with unconventional methods. I- Theoretical basis: image analysis with multivariate statistics and entropy concepts. Ultramicroscopy **34**: 165-178.

Warley A (1992) Studies on lymphocytes and thymocytes using X-ray microanalysis. In: *Electron Microscopy 1992* (Rios A, Arias JM, Megías-Megías L, eds) vol 3, Proc EUREM 92. University of Granada, Granada (Spain), pp 559-560.

Von Zglinicki T, Bimmler M (1987) The intracellular distribution of ions and water in rat liver and heart muscle. J Microsc **146**: 77-85.

Wróblewski R, Wroblewski J (1984) Freeze-drying and freeze-substitution combined with low temperature embedding. Preparation technique for microprobe analysis of biological soft tissues. Histochemistry **81**: 469-475.

Zierold K (1988) X-ray microanalysis of freeze-dried and frozen-hydrated cryosections. J Electron Microsc Techn **9**: 65-85.

Discussion with Reviewers

V. Stary: What was the experimental arrangement of temperature measurement in your system for freeze-substitution and cryoembedding. Could you give simple drawn or reference ?

Authors: The device for temperature measurement during cryoembedding, with a Pt-100 thermoresistor, is described in Figure 9 (3) by Quintana (1994). For freeze-substitution we use the same Pt-100 thermoresistor that is immersed in the glass jar containing acetone. Only when the temperature of the acetone was -90°C is the single specimen holder immersed in acetone.

V. Stary: What was the estimated thickness of sections before measurement and what was the count rate during the image acquisition ? The conditions of acquisition (200 KeV and 10ms/pixel) do not seem to be very suitable for generating pronounced element images, even though the numbers of counts (Table 7) are reasonable.

Authors: The estimated thickness was one micrometer. The conditions of acquisition at 200kV are (Table 2) 10ms per pixel per frame. The total count given in Table 7 corresponds to the set of images in Fig. 10 that were acquired with n = 12 frames, a total of 120 ms/pixel (for phosphorus the maximum total counts in 120 ms was 28 counts, that corresponds to a count rate of 233 counts per second). The set of images in Fig. 9 were acquired in 13 frames, i.e., 130 ms/pixel.

V. Stary: I did not understand exactly the information contained in the factorial images. In my opinion, the elemental content is not shown directly and only the uncorrelated parts of several elements concentrations are visible. Please explain ! In Figs. 7 and 8 you can compare directly the relations among either concentrations of various elements or different individuals (sometimes grouped according to the measured compartments). How are you able in these figures to compare simultaneously the mutual influence of both variables and individuals ?

Authors: You are right; the content of elements is only represented within the original X-ray maps (provided a background correction was performed). The factorial images do not display this content explicitly since the original X-ray maps can be considered as a linear combination of the factorial images, the coefficients of this combination being the coordinates of the chemical elements on the corresponding axes (Tables 8 and 9).

The factorial image corresponding to axis 0 is a constant (average image computed from the original X-ray maps after normalization). The factorial image corresponding to axis 1 corresponds to the first order contribution (i.e., deviation from the average) which is orthogonal to the zero-order contribution. It displays the zones of the specimen which contribute strongly (either negatively: black parts, or positively: white parts) to axis 1. The interpretation of axis 1 can be done from a chemical element point of view (example from Tables 8 and 9): P and K are correlated on axis 1), or, from a compartmental point of view (example from figure 10: axis 1 differentiates nucleic acids from the rest of the image).

The same is true for other factorial axes (hence factorial images) which are higher order (i.e., less and less important) contributions.

With these two simultaneous tools for interpretation (from the point of view of variables and from the point of view of individuals), MSA appears to be more powerful than simple (monovariate) statistical tests (e.g., correlation, Student's) concerning either the variables or

Table 10. Comparison of results obtained on cryosections with results obtained on cryoembedded specimens

	Na	*P*	*S*	*K*	*K/P*	*K/S*
NUC LIT[1,2,3]	0.015-0.03	0.23-0.47	0.03-0.23	0.38-0.48	0.84-1.7	1.6-12.4
HM23 G1[4]	0.021	0.48	0.15	0.27	0.56	1.8
HM23 G2[4]	0.07	0.49	0.12	0.21	0.43	1.7
K11M[4]	0.16	0.31	0.15	0.13	0.52	0.89
CYT LIT[1,2,3]	0.014-0.048	0.25-0.38	0.08-0.21	0.24-0.48	0.8-1.9	1.1-5.8
Cyt HM23[4]	0.06	0.29	0.22	0.29	1.0	1.4
Cyt K11M[4]	0.14	0.19	0.24	0.19	1.0	0.8
	Na/P	*Na/S*	*K/Na*	*K+Na*		
NUC LIT[1,2,3]	0.06-0.10	0.06-0.47	13.8-27.4	0.41-0.51		
HM23 G1[4]	0.04	0.14	12.8	0.29		
HM23 G2[4]	0.14	0.58	3.1	0.28		
K11M[4]	0.52	1.1	0.9	0.29		
CYT LIT[1,2,3]	0.05-0.18	0.07-0.6	10-17	0.25-0.53		
Cyt HM23[4]	0.22	0.29	4.6	0.35		
Cyt K11M[4]	0.7	0.58	1.35	0.33		

NUC LIT and CYT LIT are values for nucleus or cytoplasm, respectively, found in the literature:
[1] von Zglinicki (1987) on hydrated and freeze-dried cryosections of rat liver
[2] Somlyo (1985) on freeze-dried cryosections of rat liver
[3] Zierold (1988) on hydrated and freeze-dried cryosections of rat liver
[4] our results on CE liver and oviduct quail tissues

the individuals.

V. Stary: The hypothesis of dependence (or independence) is usually checked by some statistical tests. Are some tests usable in MSA ? What should be their results (at a known level of significance) for the described biological material or what is the level of significance of your conclusion ?

Authors: This is a difficult question to which we are not able to provide a definitive answer, because we are just beginning to explore these multivariate statistical methods for this kind of data. What we can say is that several descriptors can be used in order to check the validity of the factorial decomposition. The importance of the first eigenvalues, for instance, gives an indication of the number of factors (axes) which have to be considered.

However, concerning the level of significance of the conclusion obtained from MSA, we rely on a very empirical procedure for the moment: we just perform several similar experiments and analyses and we check whether the results (factorial decomposition and interpretation) are consistent or not. The results obtained so far are all consistent, but they cannot be considered as definitive since they are obtained from a limited number of experiments.

Reviewer II: In the introduction you state that Lowicryl resins are toxic and you say that many workers become sensitized. Could you describe their symptoms ?
Authors: The symptoms are: contact dermatitis with swollen and itching fingers, blisters, deep fissures and hyperkeratinization of the skin. Inhalation of vapor may cause irritation of eyes, mucous membrane and the upper respiratory tract (see Tobler and Freiburghaus, 1990, J Microsc **160**: 291-298).

L. Edelmann: Do you have any data of liver cryofixed by immersion in liquid propane and embedded in K11M ? Do you obtain similar results as after embedding in HM23 ?
Authors: Yes. In the first series of experiments (CE in K11M) the dissected fragments of liver and quail oviduct tissues were also cryofixed by propane immersion. The first analytical results were similar to those obtained with the Cryovacublock system: partial loss of K and increase of Na and Ca (K/Na close to 1). We did not continue to use these specimens for analysis.

V. Stary: The semi-quantitative analysis gives only concentration ratios. For estimation of the wet mass fraction you need the absolute values of concentrations (for example to check the full content of Na, Mg, P, S, Cl, K and Ca). Did you measure or estimate this absolute concentration ?
L. Edelmann: From the finding that the K/Na ratio detected after a certain cryoprocedure is the same as that known from living cells one cannot conclude that the diffusible elements are preserved at a subcellular level. Redistribution and/or loss of both elements is conceivable. Do you have experimental data showing that the K/S and Na/S ratios of different areas or whole cells are the same as obtained from freeze-dried cryosections ? (P may not be as stable as assumed in the paper).
Authors: We compared the quantitative results obtained by the Hall method on freeze-dried cryosection of liver cells with the concentrations we have obtained with our HM23 CE liver cells and K11M CE oviduct quail cells (Table 10).

The concentrations given in the literature in mmol/kg dry mass were converted into wet mass fractions (mmol/kg * molecular weight * dry fraction * 10^{-6}). We observe that the sum of concentrations (Na, Mg, P, S, Cl, K, Ca) varies between 1.79% et 0.77% [Quintana and Bonnet (1994) Scanning Microsc, in press]. In order to evaluate the concentrations in our specimens by the Cliff-Lorimer method, we have assumed a sum of concentrations for these elements equal to 1% in the different compartments. In order to compare our results with those in the literature (FD/CS samples), the sum of the concentrations **in the nuclei** of the literature data was assumed to be 1%. In this table, we observed a large dispersion of the S concentrations, and thus a large dispersion of the K/S and Na/S ratios. For HM23 CE samples, the K/S ratios are within the limits found by other authors; the Na/S values are within the limits in the group of nuclei G1 and in the cytoplasm.
Also, the (Na+K) concentration is always larger in nuclei than in the cytoplasm. We fully agree with you on the difficulty of preserving the diffusible elements at subcellular level (whatever the cryo-procedure). In our review paper (Quintana, 1994) we have written: "microanalysis at the structural level is however, problematic since there is no other technique of "in situ" ultrastructural analysis, so that element redistribution between cell compartments cannot be checked".

L. Edelmann: According to own experience (Edelmann 1989, Scanning Microscopy Suppl 3, 241-252, p 248) it is difficult (or impossible) to polymerize HM20 or HM23 in open flat embedding moulds in such way that the Lowicryl is completely left in the moulds and solid after polymerization at low temperatures (-60° to -80° C). Furthermore, even when using tightly closed embedding containers the HM23 is not solid after 1 week of polymerization at -80° C. Do you have a different experience ? Do yo use the Lowicryl mixture as recommended by the manufacturer ?
Authors: There is always volume loss of resin during the polymerization of HM23 Lowicryl in open flat embedding moulds. We have reduced this loss significantly by carefully controlling the pre-cooled nitrogen gas jet above the moulds (too strong a jet can carry away the Lowicryl, which is very fluid even at -80° C). Moreover, we used two 6 W lamps of 360 nm UV in addition to a filter for infrared (IR) and visible radiation, a very reflective polymerization chamber and small-sized moulds (high surface/volume ratio). We used the mixture recommended by the manufacturers, which we always prepared by weighing the ingredients.